Inorg. Chem. **2002**, *41*, 2761–2768

Effects of Solvents on the Electron Configurations of the Low-Spin Dicyano[*meso*-tetrakis(2,4,6-triethylphenyl)porphyrinato]iron(III) Complex: Importance of the C–H···N Weak Hydrogen Bonding

Akira Ikezaki[†] and Mikio Nakamura*[,†,‡]

Department of Chemistry, Toho University School of Medicine, Ota-ku, Tokyo 143-8540, Japan, and Division of Biomolecular Science, Graduate School of Science, Toho University, Funabashi 274-8510, Japan

Received August 6, 2001

There are two types of electron configurations, $(d_{xy})^2(d_{xz}, d_{yz})^3$ and $(d_{xz}, d_{yz})^4(d_{xy})^1$, in low-spin iron(III) porphyrin complexes. To reveal the solvent effects on the ground-state electron configurations, we have examined the ^{13}C- and ^{1}H-NMR spectra of low-spin dicyano[*meso*-tetrakis(2,4,6-triethylphenyl)porphyrinato]ferrate(III) in a variety of solvents, including protic, dipolar aprotic, and nonpolar solvents. On the basis of the NMR study, we have reached the following conclusions: (i) the complex adopts the ground state with the $(d_{xz}, d_{yz})^4(d_{xy})^1$ electron configuration, the $(d_{xz}, d_{yz})^4(d_{xy})^1$ ground state, in methanol, because the d_π orbitals are stabilized due to the O–H···N hydrogen bonding between the coordinated cyanide and methanol; (ii) the complex also exhibits the $(d_{xz}, d_{yz})^4(d_{xy})^1$ ground state in nonpolar solvents, such as chloroform and dichloromethane, which is ascribed to the stabilization of the d_π orbitals due to the C–H···N weak hydrogen bonding between the coordinated cyanide and the solvent molecules; (iii) the complex favors the $(d_{xz}, d_{yz})^4(d_{xy})^1$ ground state in dipolar aprotic solvents, such as DMF, DMSO, and acetone, though the $(d_{xz}, d_{yz})^4(d_{xy})^1$ character is less than that in chloroform and dichloromethane; (iv) the complex adopts the $(d_{xy})^2(d_{xz}, d_{yz})^3$ ground state in nonpolar solvents, such as toluene, benzene, and tetrachloromethane, because of the lack of hydrogen bonding in these solvents; (v) acetonitrile behaves like nonpolar solvents, such as toluene, benzene, and tetrachloromethane, though it is classified as a dipolar aprotic solvent. Although the NMR results have been interpreted in terms of the solvent effects on the ordering of the d_{xy} and d_π orbitals, they could also be interpreted in terms of the solvent effects on the population ratios of two isomers with different electron configurations. In fact, we have observed the unprecedented EPR spectra at 4.2 K which contain both the axial- and large g_{max}-type signals in some solvents such as benzene, toluene, and acetonitrile. The observation of the two types of signals has been ascribed to the slow interconversion on the EPR time scale at 4.2 K between the ruffled complex with the $(d_{xz}, d_{yz})^4(d_{xy})^1$ ground state and, possibly, the planar (or nearly planar) complex with the $(d_{xy})^2(d_{xz}, d_{yz})^3$ ground state.

Introduction

Two types of electron configurations, $(d_{xy})^2(d_{xz}, d_{yz})^3$ and $(d_{xz}, d_{yz})^4(d_{xy})^1$, exist in low-spin iron(III) porphyrin complexes as shown in Scheme 1.[1−3] Major factors determining the ground-state electron configurations are (i) the ligand field strength of axial ligands, (ii) the deformation mode of porphyrin rings, (iii) the electronic effects at peripheral substituents, etc.[3] Thus, while most of the low-spin complexes show the electronic ground state with the $(d_{xy})^2(d_{xz},$

* Author to whom correspondence should be addressed. E-mail: mnakamu@med.toho-u.ac.jp.
† Toho University School of Medicine.
‡ Graduate School of Science, Toho University.

(1) Walker, F. A.; Simonis, U. Proton NMR Spectroscopy of Model Hemes. In *NMR of Paramagnetic Molecules*; Berliner, L. J., Reuben, J., Eds.; Biological Magnetic Resonance; Plenum Press: New York, 1993; Vol. 12, pp 133−274.
(2) Walker, F. A. In *The Porphyrin Handbook*; Kadish, K. M., Smith, K. M., Guilard, R., Eds.; Academic Press: San Diego, CA, 2000; Chapter 36, Vol. 5, pp 81−183.
(3) Ikeue, T.; Ohgo, Y.; Saitoh, T.; Yamaguchi, T.; Nakamura, M. *Inorg. Chem.* **2001**, *40*, 3423−3434.

10.1021/ic0108383 CCC: $22.00
Published on Web 04/23/2002

Scheme 1. Extreme Electron Configurations of Low-Spin Iron(III) Porphyrin Complexes

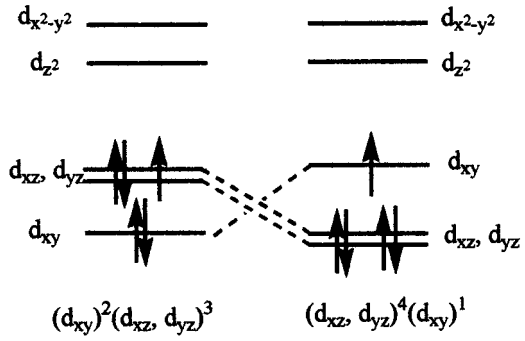

Scheme 2. Complex Examined in This Study Together with the Labeling of Carbon Atoms

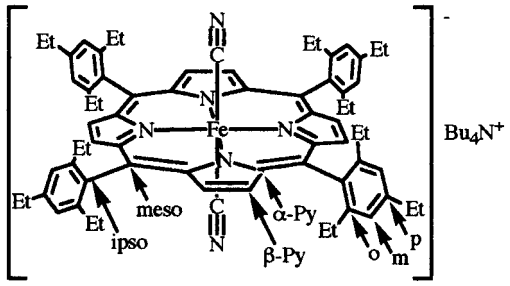

$[Fe(Et\text{-}TPP)(CN)_2]^-Bu_4N^+$

$d_{yz})^3$ configuration, the low-spin complexes that have axial ligands with low-lying π^* orbitals[4−10] and/or a highly S_4 ruffled porphyrin core exhibit the less common ground state with the $(d_{xz}, d_{yz})^4(d_{xy})^1$ configuration.[11−19] Some years ago, La Mar and co-workers pointed out that the hydrogen bonding between the coordinated cyanide and solvent molecules decreases the σ-donating and increases the π-accepting ability of the cyanide ligand.[20,21] As a result, the energy difference between the $d_\pi(d_{xz}, d_{yz})$ and d_{xy} orbitals decreases, which leads to the decrease in the magnetic anisotropy of the iron. We have recently found that, in a series of low-spin dicyano(*meso*-tetraalkylporphyrinato)-ferrate(III) complexes, the ground state with the $(d_{xz}, d_{yz})^4$-$(d_{xy})^1$ electron configuration is stabilized by the addition of methanol into the CD_2Cl_2 solutions.[13] The results have been explained in terms of the hydrogen bonding between the coordinated cyanide and methanol; that is, the O−H···N hydrogen bonding stabilizes the cyanide p_π^* orbitals which, in turn, stabilize the iron $d_\pi(d_{xz}, d_{yz})$ orbitals through the d_π−p_π^* interactions as La Mar and co-workers pointed out.[20,21] Since the role of protic solvents on the electron configuration has been clarified, our next purpose is to generalize the solvent effects on the electron configurations by using a wide range of solvents, including nonpolar solvents. We have chosen tetrabutylammonium dicyano[*meso*-tetrakis(2,4,6-triethylphenyl)porphyrinato]ferrate(III), $[Fe(Et\text{-}TPP)(CN)_2]^-Bu_4N^+$ (Scheme 2), as a model to elucidate the solvent effects, because our previous study has suggested that the energy difference between the d_π and d_{xy} orbitals is rather small.[18] This means that the small perturbation to the coordinated cyanide caused by solvents could change the energy levels of the d_π and d_{xy} orbitals of low-spin iron(III) and alter the physicochemical properties of the complex. In this paper, we report on the ground-state electron configuration of $[Fe(Et\text{-}TPP)(CN)_2]^-Bu_4N^+$ by means of the ^{13}C-NMR, ^{1}H-NMR, and EPR spectra in a variety of solvents, including protic, dipolar aprotic, and nonpolar solvents. We also report that the C−H···N weak hydrogen bonding between the coordinated cyanide and nonpolar solvents, such as chloroform and dichloromethane, plays an important role in determining the ground-state electron configuration.

Abbreviations: DMAP, 4-(*N*,*N*-dimethylamino)pyridine; DMSO, dimethyl sulfoxide; DMF, *N*,*N*-dimethylformamide; *t*-BuNC, *tert*-butyl isocyanide; HIm, imidazole; $Bu_4N^+CN^-$, tetrabutylammonium cyanide; Et-TPP, dianion of *meso*-tetrakis(2,4,6-triethylphenyl)porphyrin; TMTMP, dianion of 3,8,13,18-tetramesityl-2,7,12,17-tetramethylporphyrin; [Fe(Et-TPP)Cl], chloro[*meso*-tetrakis(2,4,6-triethylphenyl)porphyrinato]iron(III); $[Fe(Et\text{-}TPP)(CN)_2]^-Bu_4N^+$, tetrabutylammonium dicyano[*meso*-tetrakis(2,4,6-triethylphenyl)porphyrinato]ferrate(III); [Co(Et-TPP)], [*meso*-tetrakis(2,4,6-trietylphenyl)porphyrinato]cobalt(II); [Co(Et-TPP)Cl], chloro[*meso*-tetrakis(2,4,6-triethylphenyl)porphyrinato]cobalt(III); $[Co(Et\text{-}TPP)(CN)_2]^-Bu_4N^+$, tetrabutylammonium dicyano[*meso*-tetrakis(2,4,6-triethylphenyl)porphyrinato]cobaltate(III).

Experimental Section

Materials. $Bu_4N^+CN^-$ was purchased from Aldrich. Highly pure tetrachloromethane (>99.9%) was purchased from Wako. All the deuterated solvents were purchased from Merck. Deuterated solvents used in this study were methanol-d_4 (CD_3OD), dimethyl sulfoxide-d_6 (DMSO-d_6), *N*,*N*-dimethylformamide-d_7 (DMF-d_7),

(4) Simonneaux, G.; Hindre, F.; Le Plouzennec, M. *Inorg. Chem.* **1989**, *28*, 823−825.
(5) Safo, M. K.; Gupta, G. P.; Watson, C. T.; Simonis, U.; Walker, F. A.; Scheidt, W. R. *J. Am. Chem. Soc.* **1992**, *114*, 7066−7075.
(6) Safo, M. K.; Walker, F. A.; Raitsimring, A. M.; Walters, W. P.; Dolata, D. P.; Debrunner, P. G.; Scheidt, W. R. *J. Am. Chem. Soc.* **1994**, *116*, 7760−7770.
(7) Cheesman, M. R.; Walker, F. A. *J. Am. Chem. Soc.* **1996**, *118*, 7373−7380.
(8) Walker, F. A.; Nasri, H.; Turowska-Tyrk, I.; Mohanrao, K.; Watson, C. T.; Shokhirev, N. V.; Debrunner, P. G.; Scheidt, W. R. *J. Am. Chem. Soc.* **1996**, *118*, 12109−12118.
(9) Safo, M. K.; Nesset, M. J. M.; Walker, F. A.; Debrunner, P. G.; Scheidt, W. R. *J. Am. Chem. Soc.* **1997**, *119*, 9438−9448.
(10) Pilard, M.-A.; Guillemot, M.; Toupet, L.; Jordanov, J.; Simonneaux, G. *Inorg. Chem.* **1997**, *36*, 6307−6314.
(11) Nakamura, M.; Nakamura, N. *Chem. Lett.* **1991**, 1885−1888.
(12) Nakamura, M.; Ikeue, T.; Neya, S.; Funasaki, N.; Nakamura, N. *Inorg. Chem.* **1996**, *35*, 3731−3732.
(13) Nakamura, M.; Ikeue, T.; Fujii, H.; Yoshimura, T. *J. Am. Chem. Soc.* **1997**, *119*, 6284−6291.
(14) Wołowiec, S.; Latos-Grażyński, L.; Mazzanti, M.; Marchon, J.-C. *Inorg. Chem.* **1997**, *36*, 5761−5771.
(15) Wojaczyński, J.; Latos-Grażyński, L.; Glowiak, T. *Inorg. Chem.* **1997**, *36*, 6299−6306.
(16) Wołowiec, S.; Latos-Grażyński, L.; Toronto, D.; Marchon, J.-C. *Inorg. Chem.* **1998**, *37*, 724−732.
(17) Nakamura, M.; Ikeue, T.; Fujii, H.; Yoshimura, T.; Tajima, K. *Inorg. Chem.* **1998**, *37*, 2405−2414.
(18) Nakamura, M.; Ikeue, T.; Ikezaki, A.; Ohgo, Y.; Fujii, H. *Inorg. Chem.* **1999**, *38*, 3857−3862.
(19) Ikeue, T.; Ohgo, Y.; Saitoh, T.; Nakamura, M.; Fujii, H.; Yokoyama, M. *J. Am. Chem. Soc.* **2000**, *122*, 4068−4076.
(20) Frye, J. S.; La Mar, G. N. *J. Am. Chem. Soc.*, **1975**, *97*, 3561−3562.
(21) La Mar, G. N.; Gaudio, J. D.; Frye, J. S. *Biochim. Biophys. Acta* **1977**, *498*, 422−435.

acetone-d_6 ($(CD_3)_2CO$), acetonitrile-d_3 (CD_3CN), chloroform-*d* ($CDCl_3$), dichloromethane-d_2 (CD_2Cl_2), benzene-d_6 (C_6D_6), and toluene-d_8 ($C_6D_5CD_3$). Chloroform-*d* was washed several times with concentrated sulfuric acid and then with dilute sodium carbonate solution and water. It was then dried over potassium carbonate and distilled in an argon atmosphere shortly before use.[22] Other solvents were dried over an activated molecular sieve (4.0 Å) before use.

Synthesis. (Et-TPP)H_2, [Fe(Et-TPP)Cl], [Fe(Et-TPP)OAc], and [Co(Et-TPP)] were prepared according to the literature methods.[23−25] [Fe(Et-TPP)Cl]: ^{1}H-NMR (CD_2Cl_2, 25 °C, δ) 0.56 (12H, *o*-CH_3), ca. 3.0 (12H, *o*-CH_3), ca. 3.0 (8H, *o*-CH_2), 5.91 (8H, *o*-CH_2), 2.25 (12H, *p*-CH_3), 4.27 (8H, *p*-CH_2), 14.1 (4H, *m*-H), 15.7 (4H, *m*-H), 80.0 (8H, Py-H). [Fe(Et-TPP)OAc]: ^{1}H-NMR (CD_2Cl_2, 25 °C, δ) 0.36 (12H, *o*-CH_3), 1.94 (12H, *o*-CH_3), 1.94 (12H, *p*-CH_3), 3.68 (8H, *p*-CH_2), 12.69 (4H, *m*-H), 13.87 (4H, *m*-H), 78.9 (8H, Py-H), 41.0 (3H, OAc-CH_3). The *o*-methylene signals were too broad to detect. [Co(Et-TPP)]: UV−vis (CH_2Cl_2) λ_{max} (log ϵ) 414 (5.41), 531 (4.17); ^{1}H-NMR (CD_2Cl_2, 25 °C, δ) 0.82 (24H, *o*-CH_3), 3.92 (16H, *o*-CH_2), 2.56 (t, J = 7.5 Hz, 12H, *p*-CH_3), 4.22 (q, J = 7.5 Hz, 8H, *p*-CH_2), 9.20 (8H, *m*-H), 15.0 (8H, Py-H).

Synthesis of [Co(Et-TPP)Cl]. The chloroform solution (30 mL) of [Co(Et-TPP)] (150 mg) was added into an aqueous solution containing saturated sodium chloride and 1.5 g of $FeCl_3$. Bubbling of this solution with air at ambient temperature for 10 h gave [Co-(Et-TPP)Cl]. The reaction mixture was washed three times with a 1 M HCl (30 mL) solution and once with water. The pure material was obtained by the chromatography on alumina. [Co(Et-TPP)Cl]: yield, 124 mg (80%); UV−vis (CH_2Cl_2) λ_{max} (log ϵ) 411 (4.55), 551 (4.10); ^{1}H-NMR (CD_2Cl_2 δ) 0.63 (t, J = 7.5 Hz, 12H, *o*-CH_3), 0.89 (t, J = 7.5 Hz, 12H, *o*-CH_3), 1.48 (t, J = 7.6 Hz, 12H, *p*-CH_3), 1.98 (q, J = 7.5 Hz, 8H, *o*-CH_2), 2.46 (q, J = 7.5 Hz, 8H, *o*-CH_2), 2.92 (q, J = 7.6 Hz, 8H, *p*-CH_2), 7.23 (s, 4H, *m*-H), 7.31 (s, 4H, *m*-H), 8.49 (s, 8H, Py-H); ^{13}C-NMR (CD_2Cl_2 δ) 15.3 (4C, *o*-CH_3), 15.6 (4C, *o*-CH_3), 15.9 (4C, *p*-CH_3), 27.3 (4C, *o*-CH_2), 27.7 (4C, *o*-CH_2), 29.4 (4C, *p*-CH_2), 125.1 (4C, *m*), 125.5 (4C, *m*), 126.4 (4C, *meso*), 133.5 (4C, β-Py), 138.1 (4C, *ipso*), 142.4 (4C, *o*), 143.1 (4C, *o*), 145.2 (4C, *p*), 150.9 (8C, α-Py).

Synthesis of [Co(Et-TPP)(CN)$_2$]$^-$Bu$_4$N$^+$. A $CDCl_3$ solution of $Bu_4N^+CN^-$ (4.0 equiv) was added to [Co(Et-TPP)Cl] and placed in an NMR sample tube with a microsyringe to give [Co(Et-TPP)-$(CN)_2]^-Bu_4N^+$ quantitatively. ^{1}H-NMR (CD_2Cl_2 δ) 0.76 (t, J = 7.5 Hz, 24H, *o*-CH_3), 1.46 (t, J = 7.5 Hz, 12H, *p*-CH_3), 2.21 (q, J = 7.5 Hz, 16H, *o*-CH_2), 2.89 (q, J = 7.5 Hz, 8H, *p*-CH_2), 7.24 (s, 8H, *m*-H), 8.47 (s, 8H, Py-H); ^{13}C-NMR (CD_2Cl_2, δ) 15.5 (*p*-CH_3), 15.9 (*o*-CH_3), 27.8 (*p*-CH_2), 29.4 (*o*-CH_2), 115.1 (*meso*), 124.3 (*m*), 132.5 (β-Py), 137.8 (*ipso*), 143.1 (α-Py), 144.0 (*p*), 145.6 (*o*).

Spectral Measurement. ^{1}H- and ^{13}C-NMR spectra were measured on a JEOL LA300 spectrometer operating at 300.4 MHz for ^{1}H. Chemical shifts were referenced to the residual peaks of deuterated solvents. ^{1}H-NMR chemical shifts in CCl_4 were referenced to the residual peak of $CDCl_3$ placed in a capillary. EPR spectra were recorded on a Bruker E500 spectrometer operating at X band and equipped with an Oxford helium cryostat.

Sample Preparation for NMR Measurements. A $CDCl_3$ solution of $[Fe(Et\text{-}TPP)(CN)_2]^-Bu_4N^+$ (35 mM) was obtained by the addition of a 550 μL $CDCl_3$ solution of $Bu_4N^+CN^-$ (4.0 equiv) into an NMR sample tube that contained 20 mg of [Fe(Et-TPP)Cl].

Solutions of $[Fe(Et\text{-}TPP)(CN)_2]^-Bu_4N^+$ were similarly prepared in other deuterated solvents. For the signal assignments 2D HMQC and HMBC techniques were used as well as the conventional 1D spectra. ^{1}H- and ^{13}C-NMR spectra were measured at various temperatures. The temperature range examined in each solvent was as follows: CD_3OD (60 to −100 °C), $CDCl_3$ (60 to −60 °C), CD_2Cl_2 (30 to −100 °C), DMSO-d_6 (70 to 25 °C), DMF-d_7 (70 to −60 °C), $(CD_3)_2CO$ (70 to −70 °C), CD_3CN (70 to −40 °C), C_6D_6 (70 to 0 °C), $C_6D_5CD_3$ (70 to −80 °C), CCl_4 (60 to −20 °C).

Titration. A CD_2Cl_2 solution of $[Fe(Et\text{-}TPP)(CN)_2]^-Bu_4N^+$, which was prepared from [Fe(Et-TPP)Cl] (20 mg) and $Bu_4N^+CN^-$ (4.0 equiv), was titrated with acetic acid. The ^{1}H-NMR spectrum was taken to monitor the change in the pyrrole chemical shift in each case after the addition. Titration experiments with CD_3OD, $CDCl_3$, phenol, and trifluoroacetic acid were similarly done.

Results and Discussion

General Consideration. As shown in Scheme 1, there are two types of electron configurations, $(d_{xy})^2(d_{xz}, d_{yz})^3$ and $(d_{xz}, d_{yz})^4(d_{xy})^1$, in low-spin iron(III) porphyrin complexes.[1−3] If the d_{xy} orbital is located above the d_{xz} and d_{yz} orbitals (d_π orbitals) in the energy diagram, then the complex has a ground state with the $(d_{xz}, d_{yz})^4(d_{xy})^1$ electron configuration. In the following discussion, the electronic state whose ground-state configuration is $(d_{xz}, d_{yz})^4(d_{xy})^1$ or $(d_{xy})^2(d_{xz}, d_{yz})^3$ is expressed as a $(d_{xz}, d_{yz})^4(d_{xy})^1$ or $(d_{xy})^2(d_{xz}, d_{yz})^3$ ground state, respectively. Depending on the energy difference between the d_{xy} and d_π orbitals, the excited-state electron configurations contribute to the electronic state of the complex. If the d_{xy} orbital is located far above the d_π orbitals in the energy diagram, then the complex has a pure $(d_{xz}, d_{yz})^4$-$(d_{xy})^1$ ground state. On the other hand, if the energy difference is rather small, then the contribution of the excited-state electron configurations increases. The physicochemical properties of the complex, therefore, change depending on the energy difference between the d_{xy} and d_π orbitals.

In principle, a low-spin complex should adopt either the $(d_{xz}, d_{yz})^4(d_{xy})^1$ or $(d_{xy})^2(d_{xz}, d_{yz})^3$ ground state depending on the d orbital ordering determined by the ligand field strength of axial ligands, deformation of porphyrin rings, electronic effects of peripheral substituents, etc. It is possible, however, that a complex exists as the equilibrium mixture of the two isomers with the different electronic ground states; one has the $(d_{xz}, d_{yz})^4(d_{xy})^1$ ground state, while the other has the $(d_{xy})^2$-$(d_{xz}, d_{yz})^3$ ground state as shown in eq 1.

$$(d_{xy})^2(d_{xz}, d_{yz})^3 \rightleftarrows (d_{xz}, d_{yz})^4(d_{xy})^1 \qquad (1)$$

We have already reported that the ^{13}C-NMR chemical shifts of *meso* carbons are a powerful probe for determining the electronic ground state.[3,19] For example, the *meso* signal shows a large downfield shift when axially coordinated HIm is replaced by much weaker 4-CNPy in $[Fe(T^iPrP)L_2]^+$; the chemical shifts are 332 and 918 ppm at −50 °C for $[Fe(T^iPrP)(HIm)_2]^+$ and $[Fe(T^iPrP)(4\text{-}CNPy)_2]^+$, respectively.[19] The result indicates that the *$(d_{xz}, d_{yz})^4(d_{xy})^1$ character* increases on going from $[Fe(T^iPrP)(HIm)_2]^+$ to $[Fe(T^iPrP)(4\text{-}CNPy)_2]^+$,

(22) Riddick, J. A.; Bunger, W. B. *Organic Solvent, Techniques of Chemistry*; Wiley-Interscience: New York, 1970; Vol. II.
(23) Lindsey, J. S.; Wagner, R. W. *J. Org. Chem.* **1989**, *54*, 828−836.
(24) Nakamura, M.; Tajima, K.; Tada, K.; Ishizu, K.; Nakamura, N. *Inorg. Chim. Acta* **1994**, *224*, 113−124.
(25) Nakamura, M. *Bull. Chem. Soc. Jpn.* **1995**, *68*, 197−203.

Table 1. ^{13}C-NMR Chemical Shifts of $[Fe(Et\text{-}TPP)(CN)_2]^-Bu_4N^+$ Determined in Various Solvents at −20 °C

solvent	*meso*	α-Py	*β*-Py	*ipso*	*o*	*m*	*p*
CD_3OD	275.4	−17.0	76.6	68.8	236.5	130.0	146.5
$CDCl_3$	191.4	9.3	76.2	91.8	202.0	125.6	142.5
CD_2Cl_2	172.3	10.4	78.5	97.0	193.2	125.3	143.1
DMF-d_7	134.9	18.6	78.0	106.9	178.4	125.0	143.1
DMSO-d_6[a]	130.8	16.2	78.5	107.0	176.4	124.5	142.4
$(CD_3)_2CO$	123.3	20.7	77.2	109.9	174.2	124.4	142.6
CD_3CN	100.3	20.4	81.1	113.4	165.1	123.4	142.6
$C_6D_5CD_3$	96.1	25.2	80.3	116.7	164.9	123.9	142.2
C_6D_6[a]	95.5	23.8	79.6	116.1	164.5	123.7	142.1
CCl_4	79.6	25.6	82.2	119.1	158.2	122.6	140.8

[a] The value is extrapolated from high temperature.

which could be explained by either one or both of the following two ways on the basis of the discussion given above. (a) The energy gap between the d_{xy} and d_π orbitals, $\Delta E = E(d_{xy}) - E(d_\pi)$, increases on going from $[Fe(T^iPrP)(HIm)_2]^+$ to $[Fe(T^iPrP)(4\text{-}CNPy)_2]^+$. (b) The population of the isomer with the $(d_{xz}, d_{yz})^4(d_{xy})^1$ ground state is much larger in $[Fe(T^iPrP)(4\text{-}CNPy)_2]^+$ than in $[Fe(T^iPrP)(HIm)_2]^+$. In this case, the chemical shifts of the *meso* carbon signal should be given by the weighted average, as shown in eq 2, under the assumption that the interconversion is very fast on the ^{13}C-NMR time scale.

$$\delta_{obs} = x\delta(d_{xy}) + y\delta(d_\pi) \quad (2)$$

Here, δ_{obs} means the observed chemical shift of the *meso* signal, $\delta(d_{xy})$ and $\delta(d_\pi)$ are the chemical shifts of the *meso* signals in the isomers with the $(d_{xz}, d_{yz})^4(d_{xy})^1$ and $(d_{xy})^2(d_{xz}, d_{yz})^3$ ground states, respectively, and x and y are the population ratios. While a single species exists in the case of (a), two species are present in the case of (b). As mentioned later, we could actually observe two isomers at 4.2 K in frozen CH_2Cl_2 solution by EPR spectroscopy; one has the $(d_{xz}, d_{yz})^4(d_{xy})^1$ ground state, and the other has the $(d_{xy})^2(d_{xz}, d_{yz})^3$ ground state. Even in this case, the isomer with the $(d_{xz}, d_{yz})^4(d_{xy})^1$ ground state must have a large energy gap between the d_{xy} and d_π orbitals in order to explain the presence of a fairly large downfield shifted *meso* signal in $[Fe(T^iPrP)(4\text{-}CNPy)_2]^+$. In other words, even if the isomer with the $(d_{xz}, d_{yz})^4(d_{xy})^1$ ground state exists exclusively, the *meso* carbon signal does not appear at this downfield region unless the energy gap between the d_{xy} and d_π orbitals is large. For this reason, we will discuss the $(d_{xz}, d_{yz})^4(d_{xy})^1$ character in terms of the energy gap between the d_{xy} and d_π orbitals below.

Ground-State Electron Configuration of $[Fe(Et\text{-}TPP)(CN)_2]^-Bu_4N^+$. (A) ^{13}C-NMR Spectroscopy. We have established that the electronic ground state of iron(III) porphyrin complexes particularly affects the *meso* carbon chemical shifts.[3,18,19,26,27] In general, the more the $(d_{xz}, d_{yz})^4(d_{xy})^1$ ground state is stabilized, the more the spin densities at the *meso* carbon increase. Consequently, the *meso* carbon signal appears downfield. Table 1 lists the chemical shifts of the complex obtained in various solvents at −20 °C. Figure 1 shows the temperature dependence of the *meso* carbon shifts, which clearly indicates that the downfield shifts increase in the order given in eq 3.

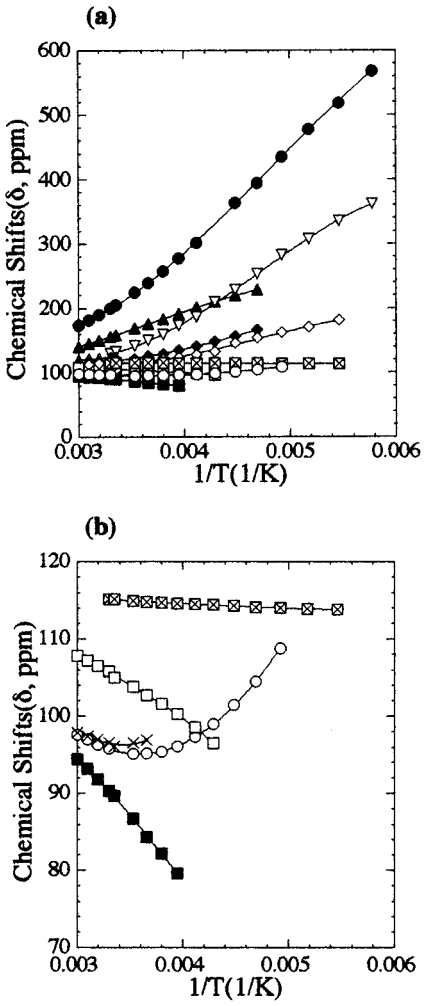

Figure 1. Temperature dependence of the ^{13}C-NMR chemical shifts of the *meso* carbon of $[Fe(Et\text{-}TPP)(CN)_2]^-Bu_4N^+$ (a) in all the solvents examined, and (b) in nonpolar solvents, such as CCl_4, C_6D_6, and $C_6D_5CD_3$, as well as in a dipolar aprotic solvent such as CD_3CN. Solvents: CD_3OD (●), $CDCl_3$ (▲), CD_2Cl_2 (▽), DMF-d_7 (♦), DMSO-d_6 (△), $(CD_3)_2CO$ (◊), CD_3CN (□), $C_6D_5CD_3$ (○), C_6D_6 (×), and CCl_4 (■). Chemical shifts of the *meso* carbon of $[Co(Et\text{-}TPP)(CN)_2]^-Bu_4N^+$ taken in CD_2Cl_2 solution (crossed box).

$$CCl_4 < C_6D_6, C_6D_5CD_3, CD_3CN < (CD_3)_2CO, \text{DMSO-}d_6, \text{DMF-}d_7 < CD_2Cl_2 < CDCl_3 < CD_3OD \quad (3)$$

Close examination of the data in Table 1 has revealed the following relationships between the *meso* carbon chemical shifts (−20 °C) and the solvents: (i) the *meso* signal appears fairly downfield, $\delta = 275$ ppm, in a protic solvent, such as methanol; (ii) large differences in chemical shifts are observed even among the nonpolar solvents; for example, the chemical shifts in $CDCl_3$ and CD_2Cl_2 are $\delta = 191$ and 172 ppm, respectively, as compared with $\delta = 80-100$ ppm in $C_6D_5CD_3$, C_6D_6, and CCl_4; (iii) the *meso* signals appear in a quite narrow range of $\delta = 129 \pm 6$ ppm, in dipolar aprotic solvents, such as DMF-d_7, DMSO-d_6, and $(CD_3)_2$-CO, which are located between those in the two types of nonpolar solvents mentioned above; (iv) the *meso* signal in

CD_3CN appears rather close to that in $C_6D_5CD_3$ or C_6D_6, ca. 100 ppm, though CD_3CN is classified as a dipolar aprotic solvent.

To obtain valuable information on the electronic ground state of low-spin iron(III) porphyrin complexes, it is necessary to extract the contact shift (δ_{con}) from the observed chemical shift (δ_{obs}).[1,2,19,28−31] The observed shift is represented as $\delta_{obs} = \delta_{dia} + \delta_{iso}$, where δ_{dia} and δ_{iso} indicate a diamagnetic and isotropic shift, respectively. Our previous work has revealed that the signs of the δ_{iso} values of *meso* carbons are different depending upon the electronic ground states; the isotropic shifts are positive (downfield shift) in the complexes with the $(d_{xz}, d_{yz})^4(d_{xy})^1$ ground state, while they are negative (upfield shift) in those complexes with the $(d_{xy})^2(d_{xz}, d_{yz})^3$ ground state.[19] Thus, the electronic ground state of the complexes could be determined by the signs of the *meso* carbon isotropic shifts. In fact, the δ_{iso} value of $[Fe(T^iPrP)(4\text{-}CNPy)_2]ClO_4$, a typical complex with the $(d_{xz}, d_{yz})^4(d_{xy})^1$ ground state, was determined to be +584 ppm,[19] while that of $[Fe(TPP)(1\text{-}MeIm)_2]Cl$, a typical complex with the $(d_{xy})^2(d_{xz}, d_{yz})^3$ ground state, was reported to be −73 ppm.[32] We have calculated the isotropic shift by using the *meso* carbon shift of $[Co(Et\text{-}TPP)(CN)_2]^-Bu_4N^+$ in CD_2Cl_2 solution as δ_{dia}; the chemical shift of the *meso* carbon is maintained almost constant at 25 °C at 115.5 ± 0.6 ppm in various solvents ranging from methanol to benzene. Thus, the linear line drawn from the temperature dependence of the *meso* carbon shift of $[Co(Et\text{-}TPP)(CN)_2]^-Bu_4N^+$ in CD_2Cl_2 solution separates the solvents where the complex adopts the $(d_{xy})^2(d_{xz}, d_{yz})^3$ ground state from those where it has the $(d_{xz}, d_{yz})^4(d_{xy})^1$ ground state, as shown in Figure 1.

To summarize the effects of solvents on the electronic ground states from the viewpoint of ^{13}C-NMR spectroscopy, it might be convenient to classify the solvents into four types: type A, protic solvents such as CD_3OD; type B, nonpolar solvents such as $CDCl_3$ and CD_2Cl_2; type C, dipolar aprotic solvents such as DMF-d_7, DMSO-d_6, and $(CD_3)_2CO$; type D, nonpolar solvents such as $C_6D_5CD_3$, C_6D_6, and CCl_4. While the complex adopts the $(d_{xz}, d_{yz})^4(d_{xy})^1$ ground state in the solvents classified as types A−C, it shows the $(d_{xy})^2(d_{xz}, d_{yz})^3$ ground state in the solvents classified as type D. Figure 1 also indicates that the $(d_{xz}, d_{yz})^4(d_{xy})^1$ character is the largest in type A solvents, followed by types B and C. It should be noted that CD_3CN is an exceptional case; the complex exhibits the $(d_{xy})^2(d_{xz}, d_{yz})^3$ ground state in this solvent, though the solvent is classified as a type C solvent.

Table 2. ^1H-NMR Chemical Shifts of $[Fe(Et\text{-}TPP)(CN)_2]^-Bu_4N^+$ Determined in Various Solvents at 25 and −20 °C

	25 °C		−20 °C	
solvent	Py-H	*m*-H	Py-H	*m*-H
CD_3OD	−6.89	8.44	−4.75	9.69
$CDCl_3$	−9.59	7.54	−9.97	8.13
CD_2Cl_2	−12.10	7.09	−12.28	7.74
DMF-d_7	−13.10	6.81	−15.28	7.05
DMSO-d_6	−12.50	7.24	−15.69[a]	7.39[a]
$(CD_3)_2CO$	−13.57	6.67	−16.11	6.91
CD_3CN	−15.07	6.52	−19.76	6.20
$C_6D_5CD_3$	−15.23	6.49	−18.66	6.63
C_6D_6	−15.06	6.50	−18.98[a]	6.41[a]
CCl_4	−15.53	6.77	−20.43	6.58

[a] The value is extrapolated from high temperature.

(B) ^1H-NMR Spectroscopy. Table 2 lists the chemical shifts of the complex taken in various solvents at 25 and −20 °C. Figure 2a,b shows the temperature dependence of the pyrrole and *meta* proton chemical shifts, respectively. In the complexes with the $(d_{xy})^2(d_{xz}, d_{yz})^3$ ground state, the unpaired electron is transferred to the β-pyrrole carbon atoms via $3e_g(porphyrin)-d_\pi(iron)$ interactions. Thus, the protons directly bonded to these carbons show significantly upfield shifted signals compared to those of the corresponding diamagnetic complex. The metal-centered dipolar shift (δ_{dip}^{MC}) also contributes, to some extent, to the upfield shift of the pyrrole signal. In the complexes with the $(d_{xz}, d_{yz})^4(d_{xy})^1$ ground state, however, the upfield shift of the pyrrole signal is reduced to a great extent due to the weakening of the $3e_g-d_\pi$ interactions. In the complexes with a pure $(d_{xz}, d_{yz})^4(d_{xy})^1$ ground state, the pyrrole signal is expected to appear close to the diamagnetic position (δ = ca. 8.5) because of the nearly zero-spin density at the β-pyrrole carbons.[19] Since the δ_{dip}^{MC} term is positive in these complexes, the pyrrole signal could appear even more downfield than that of the corresponding diamagnetic complex. In fact, $[Fe(T^iPrP)(CN)_2]^-Bu_4N^+$, which has a quite pure $(d_{xz}, d_{yz})^4(d_{xy})^1$ ground state, exhibits the pyrrole signal at δ = 12.8 ppm at −25 °C.[13] The electronic ground state can also be determined from the *meta* proton chemical shifts in the case of *meso*-tetraarylporphyrin complexes. While the complexes with the $(d_{xz}, d_{yz})^4(d_{xy})^1$ ground state show the downfield shifted *meta* signal,[18] those with the $(d_{xy})^2(d_{xz}, d_{yz})^3$ ground state exhibit the upfield shifted *meta* signal. Figure 3 shows the correlation of the chemical shifts between the pyrrole and *meta* signals in various solvents. Good linearity suggests that the chemical shifts of these signals are determined mainly by the electronic ground state of the iron(III) ion.

The following are some characteristics extracted from the data in Table 2 and Figure 2 on the relationship between the chemical shifts of the pyrrole signals at −20 °C and the solvents examined: (i) the pyrrole signal is observed at a relatively downfield region (δ = −4.5 ppm) in methanol (type A) and moves further downfield as the temperature is lowered; (ii) the pyrrole signals appear at δ = −10 to −12 ppm in nonpolar solvents such as $CDCl_3$ and CD_2Cl_2 (type

(26) Ikezaki, A.; Nakamura, M. *Chem. Lett*. **2000**, 994−995.
(27) Ikeue, T.; Ohgo, Y.; Yamaguchi, T.; Takahashi, M.; Takeda, M.; Nakamura, M. *Angew. Chem., Int. Ed.* **2001**, *40*, 2617−2620.
(28) Goff, H. In *Iron Porphyrin, Part I;* Lever, A. B. P., Gray, H. B., Eds.; Physical Bioinorganic Chemistry Series 1; Addison-Wesley: Reading, MA, 1983; pp 237−281.
(29) Bertini, I.; Luchinat, C. In *NMR of Paramagnetic Molecules in Biological Systems;* Lever, A. B. P., Gray, H. B., Eds.; Physical Bioinorganic Chemistry Series 3; Benjamin/Cummings: Menlo Park, CA, 1986; pp 165−229.
(30) Mispelter, J.; Momenteau, M.; Lhoste, J.-M. Heteronuclear Magnetic Resonance. In *NMR of Paramagnetic Molecules;* Berliner, L. J., Reuben, J., Eds.; Biological Magnetic Resonance; Plenum Press: New York, 1993; Vol. 12, pp 299−355.
(31) Bertini, I.; Luchinat, C. In *NMR of Paramagnetic Substances*; Lever, A. B. P., Ed.; Coordination Chemistry Reviews 150; Elsevier: Amsterdam, 1996; pp 29−75.
(32) Goff, H. M. *J. Am. Chem. Soc*. **1981**, *103*, 3714−3722.

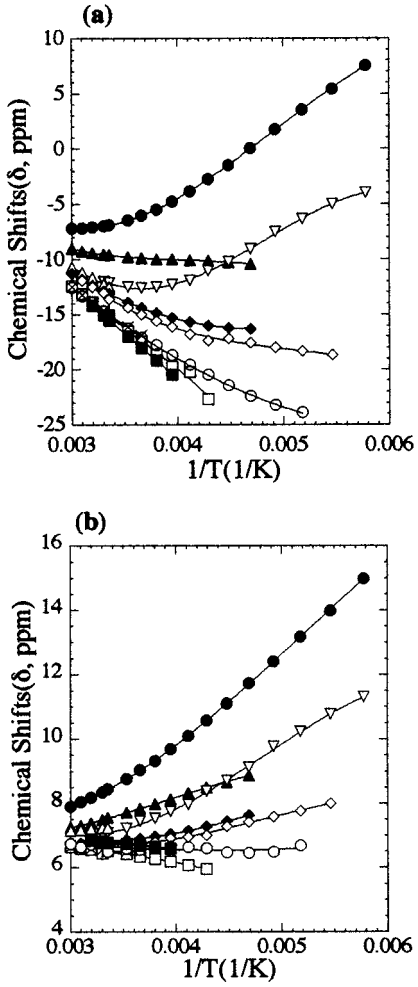

Figure 2. Temperature dependence of the ^{1}H-NMR chemical shifts of $[Fe(Et\text{-}TPP)(CN)_2]^-Bu_4N^+$ in various solvents: (a) pyrrole-H and (b) *meta*-H. Solvents measured are CD_3OD (●), $CDCl_3$ (▲), CD_2Cl_2 (▽), DMF-d_7 (♦), DMSO-d_6 (△), $(CD_3)_2CO$ (◇), CD_3CN (□), $C_6D_5CD_3$ (○), C_6D_6 (×), and CCl_4 (■).

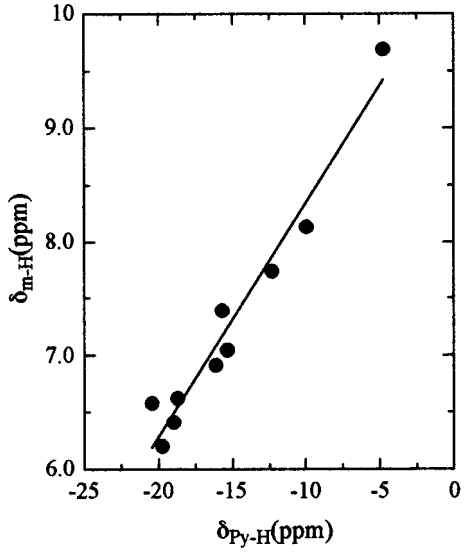

Figure 3. Correlation of the chemical shifts between the pyrrole and *meta* protons in various solvents at −25 °C (correlation coefficient, 0.956).

B), while they appear more upfield at $\delta = -19$ to -20 ppm in nonpolar solvents such as $C_6D_5CD_3$, C_6D_6, and CCl_4 (type D) (thus, the difference in chemical shifts between type B and type D solvents reaches as much as 10 ppm); (iii) the pyrrole signals are observed at $\delta = -15$ to -16 ppm in type C solvents, which are located between those signals observed in type B and type D solvents. In contrast, the pyrrole signal in CD_3CN appears at $\delta = -19.8$ ppm, which is again different from the chemical shifts in other type C solvents and close to the values in the type D solvents.

The spectral characteristics given above indicate that the complex adopts the $(d_{xz}, d_{yz})^4(d_{xy})^1$ ground state in the solvents classified as types A−C. Figure 2 also indicates that the $(d_{xz}, d_{yz})^4(d_{xy})^1$ character is the largest in type A solvents, followed by type B and type C. In contrast, in type D solvents, the complex has the $(d_{xy})^2(d_{xz}, d_{yz})^3$ ground state. Acetonitrile has exhibited unique character; the complex shows the $(d_{xy})^2$-$(d_{xz}, d_{yz})^3$ ground state in this solvent, though it is classified as a dipolar aprotic solvent (type C). Thus, the results obtained by the ^{1}H-NMR spectroscopy are totally consistent with those obtained by the ^{13}C-NMR spectroscopy.

(C) EPR Spectroscopy. Low-spin iron(III) porphyrin complexes show different EPR spectra depending on the electronic ground state.[2,33] In the case of dicyano complexes, large g_{max}-type spectra are observed if the complexes adopt the $(d_{xy})^2(d_{xz}, d_{yz})^3$ ground state. In contrast, axial-type spectra are observed if they form the $(d_{xz}, d_{yz})^4(d_{xy})^1$ ground state. Figure 4a−f shows the EPR spectra of the complex taken in various frozen solvents at 4.2 K. While the complex shows only the axial-type signals centered at $g = 2.5$ in types A−C solvents, it exhibits both the axial- ($g = 2.5$) and large g_{max}-type ($g = 3.7$) signals in type D solvents. Thus, the EPR results indicate that, while the complex adopts the $(d_{xz}, d_{yz})^4$-$(d_{xy})^1$ ground state in types A−C solvents, it exists as a mixture of two isomers with different ground states in type D solvents. Again, acetonitrile behaves like type D solvents, though it is classified as a type C solvent.

Equilibrium between the Complexes with the $(d_{xy})^2(d_{xz}, d_{yz})^3$ and $(d_{xz}, d_{yz})^4(d_{xy})^1$ Ground States. In the previous paper, we have reported that $[Fe(TMTMP)(DMAP)_2]^+ClO_4^-$ shows two kinds of EPR signals, the large g_{max}-type and rhombic-type signals, in frozen dichloromethane solution at 4.2 K.[34] The result has been explained in terms of the presence of two conformers in which only the orientation of the planar axial ligand is different; one conformer has two axial ligands oriented in a parallel fashion, while the other has two perpendicularly oriented ligands. Thus, the observation of the two types of EPR spectra has been ascribed to the slow rotation of the axial ligand on the EPR time scale at 4.2 K.

In the present study, we have observed the spectra containing both the large g_{max}-type and axial-type signals in type D solvents as well as in acetonitrile, as shown in Figure 4. The result strongly indicates that two isomers with the different ground states actually exist in frozen solution at

(33) Palmer, G. Electron Paramagnetic Resonance of Hemoproteins. In *Iron Porphyrins, Part II;* Lever, A. B. P., Gray, H. B., Eds.; Physical Bioinorganic Chemistry Series 2; Addison-Wesley: Reading, MA, 1983; pp 43−88.
(34) Ikeue, T.; Yamaguchi, T.; Ohgo, Y.; Nakamura, M. *Chem. Lett.* **2000**, 342−343.

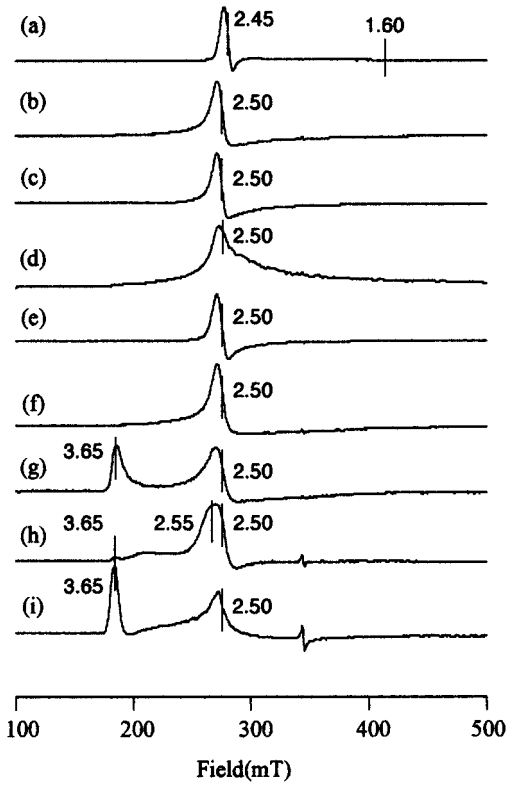

Figure 4. EPR spectra of $[Fe(Et\text{-}TPP)(CN)_2]^-Bu_4N^+$ taken in frozen solutions at 4.2 K: (a) CD_3OD, (b) $CDCl_3$, (c) CD_2Cl_2, (d) DMF-d_7, (e) DMSO-d_6, (f) $(CD_3)_2CO$, (g) CD_3CN, (h) $C_6D_5CD_3$, and (i) C_6D_6.

Scheme 3. Interconversion between the Ruffled Isomer with the $(d_{xz}, d_{yz})^4(d_{xy})^1$ Ground State and the Planar (or Nearly Planar) Isomer with the $(d_{xy})^2(d_{xz}, d_{yz})^3$ Ground State

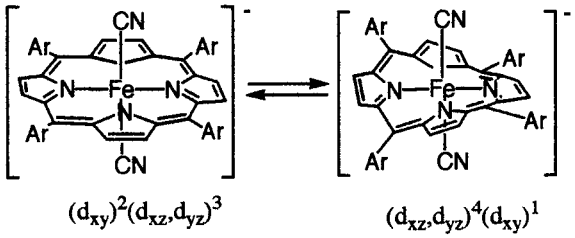

4.2 K, and that the mutual exchange between these two isomers is slow on the EPR time scale at this temperature. Since the complexes with the $(d_{xz}, d_{yz})^4(d_{xy})^1$ ground state always exhibit the ruffled porphyrin ring,[2] the observation of the two isomers should be ascribed to the high barrier to interconversion between the ruffled complex with the $(d_{xz}, d_{yz})^4(d_{xy})^1$ ground state and, possibly, the planar (or nearly planar) complex with the $(d_{xy})^2(d_{xz}, d_{yz})^3$ ground state, as shown in Scheme 3.

Hydrogen Bonding between Coordinated Cyanide and Acids. As shown in Figure 5, the pyrrole proton signal moves downfield if compounds such as acetic acid, phenol, methanol, and chloroform are added to a $[Fe(Et\text{-}TPP)(CN)_2]Bu_4N^+$-solution. The result suggests that the $(d_{xz}, d_{yz})^4(d_{xy})^1$ character increases as the acid is added due to the stabilization of the d_π orbitals caused by the hydrogen bonding between the acid and the coordinated cyanide. In the case of acetic acid, the signal intensity of $[Fe(Et\text{-}TPP)(CN)_2]^-Bu_4N^+$ decreases when more than 5.0 equiv of the acid is added. Instead, the signals ascribed to [Fe(Et-TPP)Cl] and [Fe(Et-TPP)OAc] increase.

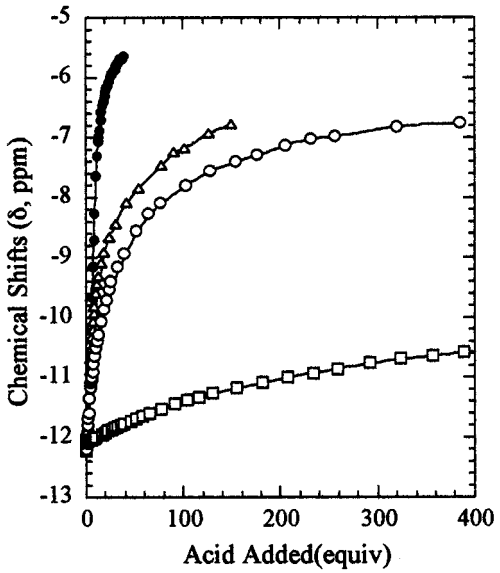

Figure 5. Change in ^{1}H-NMR pyrrole shift against the amount of the acid added. Each acid was added to a solution containing $[Fe(Et\text{-}TPP)(CN)_2]^-Bu_4N^+$ and CN^- in 1:2 molar ratios at 25 °C: CH_3COOH (●), C_6H_5OH (△), CD_3OD (○), and $CDCl_3$ (□).

Scheme 4. (a) Structural Formula of Alkyl or Aryl Isocyanide and (b) Resonance Presentation of the Hydrogen Bonding between Proton Donor and Cyanide[a]

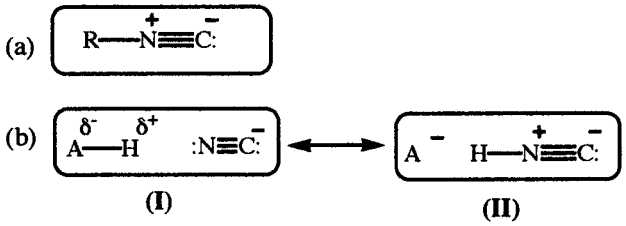

[a]Note that the resonance structure (**II**) is quite similar to the isocyanide.

After the addition of more than 40 equiv of the acid, $[Fe(Et\text{-}TPP)(CN)_2]^-Bu_4N^+$ is completely converted to [Fe(Et-TPP)Cl] and [Fe(Et-TPP)OAc], as is revealed by the ^{1}H-NMR spectra.

Similar changes in the pyrrole shift are observed by the addition of much weaker acids such as phenol and methanol, though the downfield shift is not as large as in the case of acetic acid. These results indicate that the hydrogen bonding to the coordinated cyanide weakens the σ-donating and strengthens the π-accepting ability of the coordinated cyanide ligand as La Mar and co-workers pointed out. Thus, the $(d_{xz}, d_{yz})^4(d_{xy})^1$ ground state is stabilized in the presence of phenol and methanol.[13,20,21] Scheme 4 shows the resonance structures of the hydrogen-bonded cyanide ligand. In the presence of a strong acid, the resonance structure (**II**) becomes the major contributor. Since **II** is supposed to be quite similar to alkyl or aryl isocyanide (R−NC) in its electronic structure, the $(d_{xz}, d_{yz})^4(d_{xy})^1$ ground state is greatly stabilized, as in the case of bis(R−NC) complexes; all the bis(R−NC) complexes reported previously show a very pure $(d_{xz}, d_{yz})^4(d_{xy})^1$ ground state due to the weak σ-donating and fairly strong π-accepting ability.[3,4,8,35,36]

Weak Hydrogen Bonding between Coordinated Cyanide and $CDCl_3$ or CD_2Cl_2. We have mentioned that the

chemical shifts of the pyrrole proton and *meso* carbon signals are greatly affected by the nature of the solvents; the signals appear more downfield in CD_3OD than in C_6D_6 and CCl_4. Surprisingly, the chemical shifts are very much different even among the nonpolar solvents. That is, while the *meso* carbon signals appear at 170−190 ppm at −20 °C in type B solvents, such as CD_2Cl_2 and $CDCl_3$, they appear at 80−100 ppm in type D solvents, such as $C_6D_5CD_3$, C_6D_6, and CCl_4. Furthermore, the temperature dependence is very much different between these two types of nonpolar solvents as shown in Figure 1a,b. Thus, the chemical shift in CD_2Cl_2 differs from that in $C_6D_5CD_3$ by as much as 170 ppm at −70 °C! The difference in chemical shifts is also observed in the pyrrole protons; the pyrrole signal appears at −7.5 ppm at −70 °C in CD_2Cl_2 in contrast to the signal at −23.2 ppm in $C_6D_5CD_3$.

In the previous section, we pointed out that the addition of acids, such as acetic acid, phenol, and even methanol, into a CD_2Cl_2 solution of $[Fe(Et\text{-}TPP)(CN)_2]^-Bu_4N^+$ stabilizes the $(d_{xz}, d_{yz})^4(d_{xy})^1$ ground state via the O−H···N hydrogen bonding with the coordinated cyanide ligand.[13,20,21] As shown in Figure 5, the addition of $CDCl_3$ to a CD_2Cl_2 solution of the complex also induces a downfield shift. The result suggests that the C−H···N weak hydrogen bonding exists even between the coordinated cyanide and chloroform molecules.[37] The smaller amount of the downfield shift in chloroform as compared with methanol indicates that chloroform is much weaker than methanol in proton donor ability. Many examples have been reported on the C−H···X type hydrogen bonding in the crystal.[37−39] Chloroform is known to be a much stronger proton donor than other compounds having C−H bonds on the basis of the C−H···X distances in the crystal.[40−43] Formation of the C−H···X hydrogen bonding is also reported for dichloromethane in the crystal.[43] The presence of the C−H···X hydrogen bonding has been reported even in solution between chloroform and pyridine or between chloroform and DMSO.[44] Thus, it must be a reasonable assumption to ascribe the stabilization of the $(d_{xz}, d_{yz})^4(d_{xy})^1$ ground state in $CDCl_3$ and CD_2Cl_2 to the C−D···N weak hydrogen bonding between the coordinated cyanide and solvent molecules.

Effects of Dipolar Aprotic Solvents on the Electronic Ground State. In dipolar aprotic solvents (type C solvents), the chemical shifts of the *meso* carbon and pyrrole proton signals are located between those obtained in the two types of nonpolar solvents, types B and D. On the basis of the NMR results, it is concluded that the energy gap between the d_{xy} and d_π orbitals in type C solvents is less than that in type B solvents, which should be ascribed to the difference in proton donor ability among these solvents. As mentioned in a previous section (General Consideration), it should be noted here that the results could be explained differently; that is, the populations of the isomer with the $(d_{xz}, d_{yz})^4(d_{xy})^1$ ground state are much larger in type B solvents as compared with those in type C solvents due to the hydrogen bonding. The proton donor ability is estimated by the C−H···X (X = N, O, or Cl^-) bond distances in the crystal.[40−43] In fact, the X-ray crystallographic studies have revealed that the C−H···X bond distances of acetonitrile, DMSO, and acetone are longer than those of chloroform and dichloromethane, supporting the hypothesis mentioned above.[43] Among the type C solvents examined in this study, CD_3CN differs from the others and resembles the type D solvents. In fact, the chemical shifts of the *meso* carbons are 96.5 and 99.0 ppm in CD_3CN and $C_6D_5CD_3$, respectively, at −40 °C. Similarly, the EPR spectrum in frozen CD_3CN shows both the axial- and large g_{max}-type signals, as in the case of C_6D_6 solutions. Thus, CD_3CN behaves like type D solvents, which could be ascribed to the weak proton donor ability.

Acknowledgment. This work was supported by a Grant in Aid (12020257) for Scientific Research on Priority Areas (A) (to M.N.) from the Ministry of Education, Culture, Sports, Science and Technology, Japan, and by the Nukada Fund for the Advancement of Science of Toho University (to A.I.). Thanks are due to the Research Center for Molecular Materials, the Institute for Molecular Science (IMS).

Supporting Information Available: ^{1}H-NMR and ^{13}C-NMR spectra of $[Fe(Et\text{-}TPP)(CN)_2]Bu_4N$ in CD_2Cl_2 solution. This material is available free of charge via the Internet at http://pubs.acs.org.

IC0108383

(35) Simonneaux, G.; Schünemann, V.; Morice, C.; Carel, L.; Toupet, L.; Winkler, H.; Trautwein, A. X.; Walker, F. A. *J. Am. Chem. Soc.* **2000**, *122*, 4366−4377.
(36) Simonneaux, G.; Kobeissi, M. *J. Chem. Soc., Dalton Trans.* **2001**, 1587−1592.
(37) Desiraju, G. R.; Steiner, T. The Weak Hydrogen Bond. In *Structural Chemistry and Biology*; Oxford University Press: New York, 1999.
(38) Sutor, D. J. *J. Chem. Soc.* **1963**, 1105−1110.
(39) Steiner, T. *Chem. Commun.* **1997**, 727−734.
(40) Desiraju, G. R. *J. Chem. Soc., Chem. Commun.* **1989**, 179−180.
(41) Pedireddi, V. R.; Desiraju, G. R. *J. Chem. Soc., Chem. Commun.* **1992**, 988−990.
(42) Steiner, T. *J. Chem. Soc., Chem. Commun.* **1994**, 2341−2342.
(43) Steiner, T. *New J. Chem.* **1998**, 1099−1103
(44) Allerhand, A.; Schleyer, P. v. R. *J. Am. Chem. Soc.* **1963**, *85*, 1715−1723.